

# Phosphinodi(benzylsilane) $\text{PhP}\{(o\text{-C}_6\text{H}_4\text{CH}_2)\text{SiMe}_2\text{H}\}_2$ : A Versatile "PSi<sub>2</sub>H<sub>x</sub>" Pincer-Type Ligand at Ruthenium

Virginia Montiel-Palma,<sup>\*,†</sup> Miguel A. Muñoz-Hernández,<sup>†</sup> Cynthia A. Cuevas-Chávez,<sup>†</sup> Laure Vendier,<sup>‡,§</sup> Mary Grellier,<sup>‡,§</sup> and Sylviane Sabo-Etienne<sup>\*,‡,§</sup>

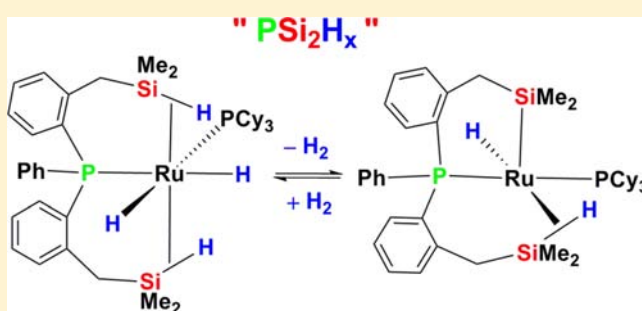
<sup>†</sup>Centro de Investigaciones Químicas, Universidad Autónoma del Estado de Morelos, Avenida Universidad 1001, Col. Chamilpa, Cuernavaca, Morelos, C. P. 62209, México

<sup>‡</sup>CNRS, LCC (Laboratoire de Chimie de Coordination), 205 route de Narbonne, BP 44099, F-31077 Toulouse Cedex 4, France

<sup>§</sup>Université de Toulouse, UPS, INPT, F-31077 Toulouse Cedex 4, France

## Supporting Information

**ABSTRACT:** The synthesis of the new phosphinodi(benzylsilane) compound  $\text{PhP}\{(o\text{-C}_6\text{H}_4\text{CH}_2)\text{SiMe}_2\text{H}\}_2$  (**1**) is achieved in a one-pot reaction from the corresponding phenylbis(*o*-tolylphosphine). Compound **1** acts as a pincer-type ligand capable of adopting different coordination modes at Ru through different extents of Si–H bond activation as demonstrated by a combination of X-ray diffraction analysis, density functional theory calculations, and multinuclear NMR spectroscopy. Reaction of **1** with  $\text{RuH}_2(\text{H}_2)_2(\text{PCy}_3)_2$  (**2**) yields quantitatively  $[\text{RuH}_2\{\{\eta^2\text{-}(\text{HSiMe}_2)\text{-CH}_2\text{-}o\text{-C}_6\text{H}_4\}_2\text{PPh}\}(\text{PCy}_3)]$  (**3**), a complex stabilized by two rare high order  $\epsilon$ -agostic Si–H bonds and involved in terminal hydride/ $\eta^2$ -Si–H exchange processes. A small free energy of reaction ( $\Delta_r G_{298} = +16.9 \text{ kJ mol}^{-1}$ ) was computed for dihydrogen loss from **3** with concomitant formation of the 16-electron species  $[\text{RuH}\{\{\eta^2\text{-}(\text{HSiMe}_2)\text{-CH}_2\text{-}o\text{-C}_6\text{H}_4\}_2\text{PPh}\}[\text{CH}_2\text{-}o\text{-C}_6\text{H}_4\text{SiMe}_2]\}(\text{PCy}_3)]$  (**4**). Complex **4** features an unprecedented <sup>29</sup>Si NMR decoalescence process. The dehydrogenation process is fully reversible under standard conditions (1 bar, 298 K).



## INTRODUCTION

The use of multidentate ligands in transition-metal chemistry offers widespread applications due to the possibility of varying the anchoring points and thus modulating the properties of the metal center. Recently, the design of “cooperating” ligands led to remarkable improvements in catalysis as illustrated in particular by aromatization–dearomatization processes.<sup>1,2</sup> Silicon is a strong  $\sigma$  donor and exerts a strong trans influence,<sup>3</sup> and these properties make it an excellent choice for incorporation into the skeleton of multidentate ligands.<sup>4–6</sup> Indeed, there is an increasing number of reports of phosphorus–silicon multidentate ligands stemming from the pioneering work of Stobart.<sup>7</sup> These studies have demonstrated different degrees of reactivity control resulting in unusual activation or properties,<sup>8–18</sup> together with enhanced catalytic behavior.<sup>19–21</sup> These systems feature only one Si in combination with either one, two, or three phosphorus atoms. However, the presence of two Si atoms in bis(silyl) systems is known to induce specific properties with a major influence in catalysis.<sup>22–24</sup> Recently, Driess and Hartwig reported how the presence of two Si in bis(silylene) SiCHSi pincer ligands resulted in significant reactivity and selectivity changes in catalytic C–H borylation of arenes with respect to other bidentate nitrogen ligands in Pd<sup>25</sup> and Ir<sup>26</sup> systems. The SiCSi ligand showed a stronger  $\sigma$ -donor capability than

analogous P<sup>III</sup> pincer species. In this context, the design of silicon pincer-type ligands featuring Si–H bonds for “cooperating” effects seemed highly relevant. We have previously explored the reactivity of two phosphinosilane compounds with ruthenium precursors and observed a versatile coordination chemistry. The phosphinobenzylsilane ligand  $\text{Ph}_2\text{P}(o\text{-C}_6\text{H}_4)\text{CH}_2\text{SiMe}_2\text{H}$  led to a complex displaying two rare high-order  $\epsilon$ -agostic Si–H bonds, which, upon stepwise H<sub>2</sub> loss through C–H activation, produced a bis  $\beta$ -agostic Si–H species with two carbon–metalated bonds.<sup>8</sup> In the case of  $\text{Ph}_2\text{PCH}_2\text{OSiMe}_2\text{H}$ , we isolated a complex containing three phosphinosilane ligands each adopting a different coordination mode to Ru.<sup>13</sup> Reported herein is the synthesis of the phosphinodi(benzylsilane) compound  $\text{PhP}\{(o\text{-C}_6\text{H}_4\text{CH}_2)\text{SiMe}_2\text{H}\}_2$  (**1**) and its reactivity toward the bis(dihydrogen) ruthenium complex  $\text{RuH}_2(\text{H}_2)_2(\text{PCy}_3)_2$  (**2**). The new phosphinodibenzylsilane compound  $\text{PhP}\{(o\text{-C}_6\text{H}_4\text{CH}_2)\text{SiMe}_2\text{H}\}_2$  acts as a pincer-type ligand “PSi<sub>2</sub>H<sub>x</sub>” capable of adopting different coordination modes at ruthenium through different extents of Si–H bond activation.

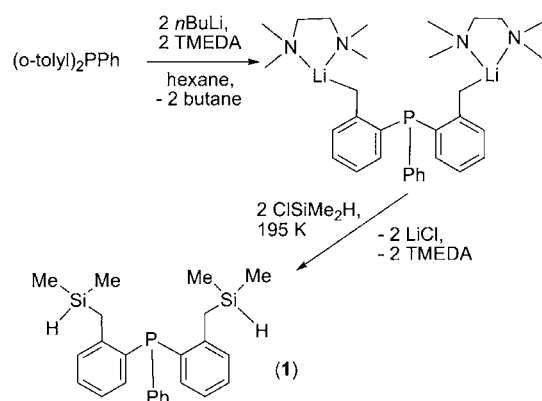
Received: March 22, 2013

Published: August 13, 2013

## RESULTS AND DISCUSSION

**Synthesis and Characterization of the Phosphinodi-(Benzylsilane)  $\text{PhP}\{(o\text{-C}_6\text{H}_4\text{CH}_2\text{SiMe}_2\text{H})_2\}$  (1) and of the Ruthenium Complex  $[\text{RuH}_2\{[\eta^2\text{-(HSiMe}_2\text{)-CH}_2\text{-}o\text{-C}_6\text{H}_4\text{]}_2\text{-PPH}\{\text{PCy}_3\}]$  (3).** The new phosphinodi(benzylsilane) **1** was prepared in 83% yield in a one-pot reaction from dilithiation of  $\text{PhP}(o\text{-tolyl})_2$  with  $n\text{BuLi}$  in the presence of TMEDA followed by addition of  $\text{ClMe}_2\text{SiH}$  (Scheme 1). Its main NMR

**Scheme 1. Synthesis of the Phosphinodi(Benzylsilane) Compound 1**

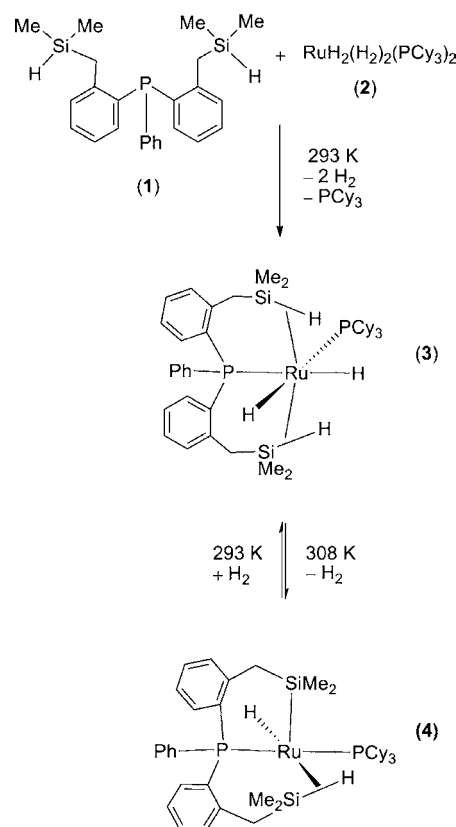


spectroscopic features are  $^1\text{H}$  signals at  $\delta$  4.21 (multiplet) for the H–Si and at  $\delta$  2.44 and  $\delta$  0.5 for the methylene and methyl groups respectively. At 700 MHz, two diastereotopic environments are confirmed for the methyl hydrogens as two sets of doublets of doublets with the larger constant due to Si–H coupling ( $^3J_{\text{HH}}$  3.5 Hz). The diastereotopicity of the methylene hydrogens is barely distinguishable as two doublets separated by less than 2 Hz with the resolved coupling also due to Si–H coupling. The  $^{31}\text{P}$  and  $^{29}\text{Si}$  signals appear at  $\delta$  –21.1 and  $\delta$  –11.5 ( $^1J_{\text{Si-H}}$  196 Hz), respectively. Compound **1** reacts at room temperature in benzene- $d_6$ , toluene- $d_8$ , or THF with the bis(dihydrogen) complex **2** affording compound **3** as a result of the formal substitution of the two dihydrogen and one tricyclohexylphosphine ligands of **2** by the phosphinodi-(benzylsilane) ligand (Scheme 2).

Crystals of **3** suitable for X-ray diffraction analysis were grown under 3 bar of dihydrogen from concentrated benzene- $d_6$  solutions of in situ generated **3**. Two highly similar crystallographically independent molecules were found in the unit cell. For simplicity, and because one molecule presents positional disorder in one of the cyclohexyl rings of the coordinated  $\text{PCy}_3$  ligand, only the structural features of the nondisordered molecule will be further discussed. The molecular structure of **3** is shown in Figure 1, and relevant bond lengths and angles are presented in Table 1.

The ruthenium center adopts a pseudo-octahedral environment. The central phosphorus atom of the coordinated phosphinodi(benzylsilane) ligand and the  $\text{PCy}_3$  ligand display a rather acute P–Ru–P angle of  $113.32(4)^\circ$ . A *cis* disposition for bulky phosphine ligands is not without precedent in ruthenium chemistry. In particular, the disilane complexes  $[\text{RuH}_2\{[\eta^2\text{-(HSiMe}_2\text{)}_2\text{X}]\{\text{PCy}_3\}_2]$  ( $\text{X} = \text{C}_6\text{H}_4, \text{CH}_2\text{CH}_2, \text{OSiMe}_2\text{O}$ )<sup>27</sup> generated from the reaction of **2** with the corresponding disilanes  $(\text{HSiMe}_2)_2\text{X}$  exhibit *cis*-phosphines with P–Ru–P angles close to  $108^\circ$  as a result of increased stabilization owing to the establishment of secondary

**Scheme 2. Reactivity of 1 with 2 Generating 3 and 4 in Subsequent Reaction Steps**



interactions between the terminal hydrides and the Si atoms (SISHA).<sup>28,29</sup> In complex **3**, the X spacer is now a dibenzylphosphino group, allowing the formation of a pincer-type ligand if one considers the phosphorus and the middle of the two Si–H bonds coordinated to ruthenium. A large distortion is imposed by the silicon atoms bending away from each other to  $112.36(5)^\circ$ . To describe the binding mode of the two Si and four H atoms around the Ru center, one could in principle envisage three extreme structures. A structure resulting from the oxidative addition of the two Si–H bonds can be immediately discarded, as a tetrahydride(disilyl) Ru(VI) formulation is unrealistic. Alternatively, the two Si–H bonds coordinate to Ru in a nonclassical fashion, thus leading formally to a dihydride bis( $\eta^2\text{-Si-H}$ ) Ru(II) species **3a**, or only one of the Si–H bonds is  $\eta^2$ -coordinated to Ru, whereas the second is fully activated generating a trihydride mono( $\eta^2\text{-Si-H}$ ) Ru(IV) species **3b** (Scheme 3). Bearing in mind the uncertainties in the hydride location by X-ray diffraction, two elongated bonding Si–H distances are found in the structure of **3**: Si1–H100 and Si2–H101 at 1.62(4) and 1.68(4) Å, respectively. The four Ru–H bond distances are rather undifferentiated lying in the range 1.53–1.59 Å. All but one of the hydrogens bound to Ru, H102, can be accommodated in a plane together with the Ru and the two silicon atoms; out-of-plane H102 lies almost *trans* to the bridgehead P of the pincer ligand, while in-plane H103 is approximately *trans* to  $\text{PCy}_3$ . Additional secondary interactions (SISHA) between the silicons and H103 can be evidenced by distances in the typical range 1.9–2.4 Å. The distances determined by X-ray diffraction are consistent with the **3a** formulation. To overcome the experimental ambiguities brought by the X-ray location of the hydride ligands, DFT/

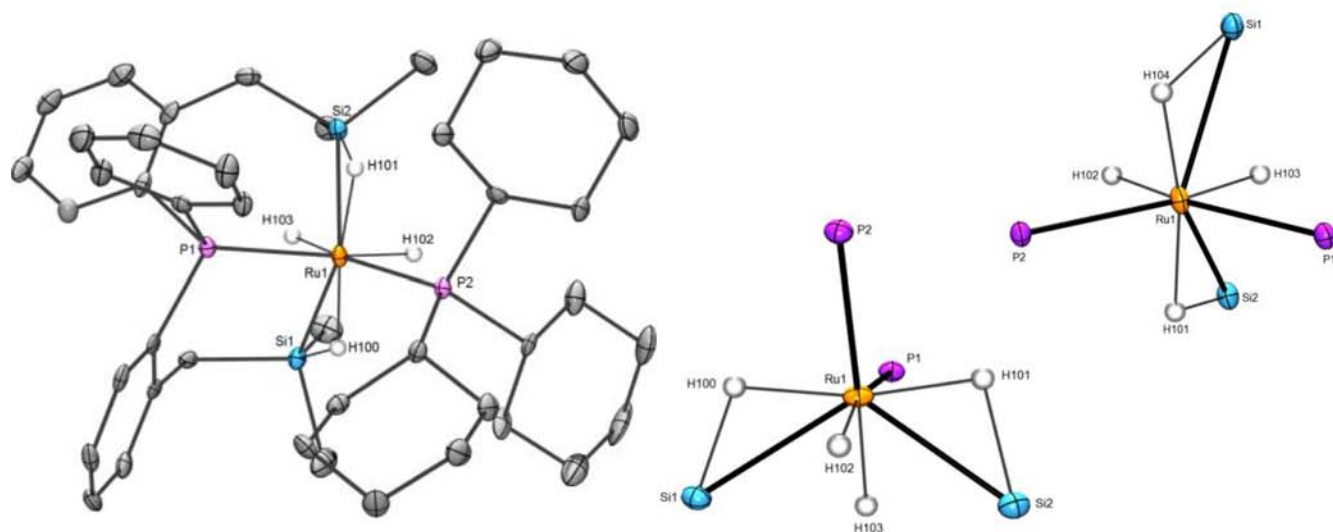


**Figure 1.** (Left) X-ray diffraction structure of **3** with thermal ellipsoids at the 50% probability level; most hydrogen atoms were removed for clarity. (Center/right) Views showing the close to *cis* disposition of the phosphorus and silicon atoms. The plane containing the two phosphorus and the two hydrides is nearly perpendicular to that of the two  $\eta^2$ (Si–H) ligands (right) allowing for SISHA interactions to take place. All carbon and most hydrogen atoms were removed for clarity.

**Table 1. Selected Bond Lengths (Å) and Angles (°) for Complexes **3** and **4** (X-ray) and Their Calculated Counterparts (DFT/B3PW91)**

	<b>3</b> (X-ray)	<b>3cis</b> (DFT)	<b>4</b> (X-ray)	<b>4</b> (DFT)
Ru–P1	2.376 (1)	2.413	2.308(1)	2.353
Ru–P2	2.392 (1)	2.419	2.346(1)	2.375
Ru–Si1	2.542(2)	2.613	2.473(1)	2.523
Ru–Si2	2.420(1)	2.419	2.324(1)	2.352
Si1–H100	1.62(4)	1.659	1.71(3)	1.763
Si2–H101	1.68(4)	1.889		2.800
Si2–H103		2.064		
Si1–H103		2.309		
P1–Ru–P2	113.32(4)	114.4	154.37(3)	152.5
Si1–Ru–Si2	112.36(5)	115.3	104.50(4)	101.7
P1–Ru–Si1	91.70(5)	90.8	87.15(3)	86.3
P1–Ru–Si2	95.16(5)	95.5	88.66(3)	89.2
P2–Ru–Si1	118.80(5)	116.1	113.42(3)	113.9
P2–Ru–Si2	119.14(5)	118.8	100.02(3)	103.6

B3PW91 calculations were carried out without any simplification of the ligands. Two isomers, **3cis** and **3trans** have been characterized on the potential energy surface. The lowest in energy, **3cis**, displays a geometry closely resembling that determined by X-ray diffraction, and the results show an excellent agreement between both methods (Table 1). In particular, the two Si–H bond distances are typical of  $\eta^2$ -Si–H bonds within the range 1.6–1.9 Å, with the H atoms almost *trans* to each other. Two nonbonding Si···H distances are characteristic of SISHA interactions, Si2···H103 2.064 Å and Si1···H103 2.309 Å. Finally, the Ru–Si distances are very good indicators of the degree of activation of the Si–H bonds. Although one of the two Si is closer to Ru (X-ray: 2.420(1) vs 2.542(2) Å, DFT: 2.419 vs 2.613 Å), the two bond distances lie within the range generally accepted for nonclassical  $\eta^2$ -Si–H bonds.<sup>23</sup> These findings are in accordance with the nonclassical character of the two Si–H bonds, and the complex can be formulated in the solid state as the dihydride species  $[\text{RuH}_2\{\{\eta^2\text{-(HSiMe}_2\text{)-CH}_2\text{-}o\text{-C}_6\text{H}_4\}_2\text{PPh}\}(\text{PCy}_3)]$  stabilized

by two rare high order  $\epsilon$ -agostic Si–H interactions with additional SISHA interactions.<sup>25</sup>

At 293 K, the  $^1\text{H}$  NMR spectrum of **3** in toluene- $d_8$  displays one broad signal in the hydride region integrating for four hydrogen atoms at  $\delta$  –9.02, which remains broad even at the lowest accessible temperature (193 K). At 263 K, the HMQC  $^1\text{H}$ – $^{29}\text{Si}\{\text{P}\}$  NMR spectrum shows a  $^{29}\text{Si}$  signal at  $\delta$  –0.7 correlating with the  $^1\text{H}$  signal at  $\delta$  –9.02 with an apparent  $J_{\text{Si-H}}$  coupling constant of 40 Hz. The  $J_{\text{Si-H}}$  coupling constant value is a highly valuable tool for assessing the extent of nonclassical interactions, this value being very small for silyl hydrides, typically fewer than 20 Hz, while between 40–80 Hz for nonclassical  $\eta^2$ -SiH interactions.<sup>23,29–31</sup> However, due to sign uncertainties, care must be taken when using these coupling constants as indicators of the strength of the interaction between the atoms.<sup>23,32</sup> The  $T_{1\text{min}}$  value of 373 ms at 273 K and 500 MHz is too long to postulate a dihydrogen formulation. In the  $^{31}\text{P}\{\text{H}\}$  NMR spectrum, two doublets corresponding to an AX spin system pattern are observed at  $\delta$  29.7 for the phosphinodi(benzylsilane) and  $\delta$  68.3 for the coordinated  $\text{PCy}_3$  with a  $^2J_{\text{P-P}}$  coupling constant of 121 Hz. This latter value is significantly larger than those obtained for  $[\text{RuH}_2\{\{\eta^2\text{-HSiMe}_2\}_2\text{X}\}(\text{PCy}_3)(\text{PR}_3)]$  (with X =  $\text{C}_6\text{H}_4$ ,  $(\text{CH}_2)_2$ ,  $(\text{CH}_2)_3$ ,  $\text{OSi}(\text{Me}_2)\text{O}$  and R = Ph, pyl), which are in the range 20–30 Hz.<sup>27</sup> It is however considerably smaller than that reported for  $[\text{RuH}_2\{\{\eta^4\text{-HSiMe}_2(\text{CH}=\text{CHMe})\}(\text{PCy}_3)_2\}]$  ( $^2J_{\text{P-P}}$  206 Hz) related to a P–Ru–P angle of 145.30(6)°.<sup>33</sup> The diminished  $^2J_{\text{P-P}}$  coupling constant is in accordance with a stereochemistry in which the phosphorus atoms are intermediate between *cis* and *trans* disposition. In addition, the  $^{31}\text{P}$  NMR spectrum of a reaction mixture of in situ generated **3** and  $\text{PCy}_3$  at 293 K (from the reaction mixture of **1** and **2** in a 2:1 mol equivalent ratio in a Young's tap NMR tube) shows exchange of the Ru-coordinated  $\text{PCy}_3$  ligand with free  $\text{PCy}_3$ , which is halted by lowering the temperature. The high fluxionality of **3** is in contrast with the observed behavior of the aforementioned disilane complexes  $[\text{RuH}_2\{\{\eta^2\text{-HSiMe}_2\}_2\text{X}\}(\text{PCy}_3)_2]$  (X =  $\text{C}_6\text{H}_4$ ,  $\text{CH}_2\text{CH}_2$ ,  $\text{OSi}(\text{Me}_2)\text{O}$ ), all of which exhibit two resonances in the hydride region at ambient

Scheme 3. Possible Arrested Structures for 3 and 4

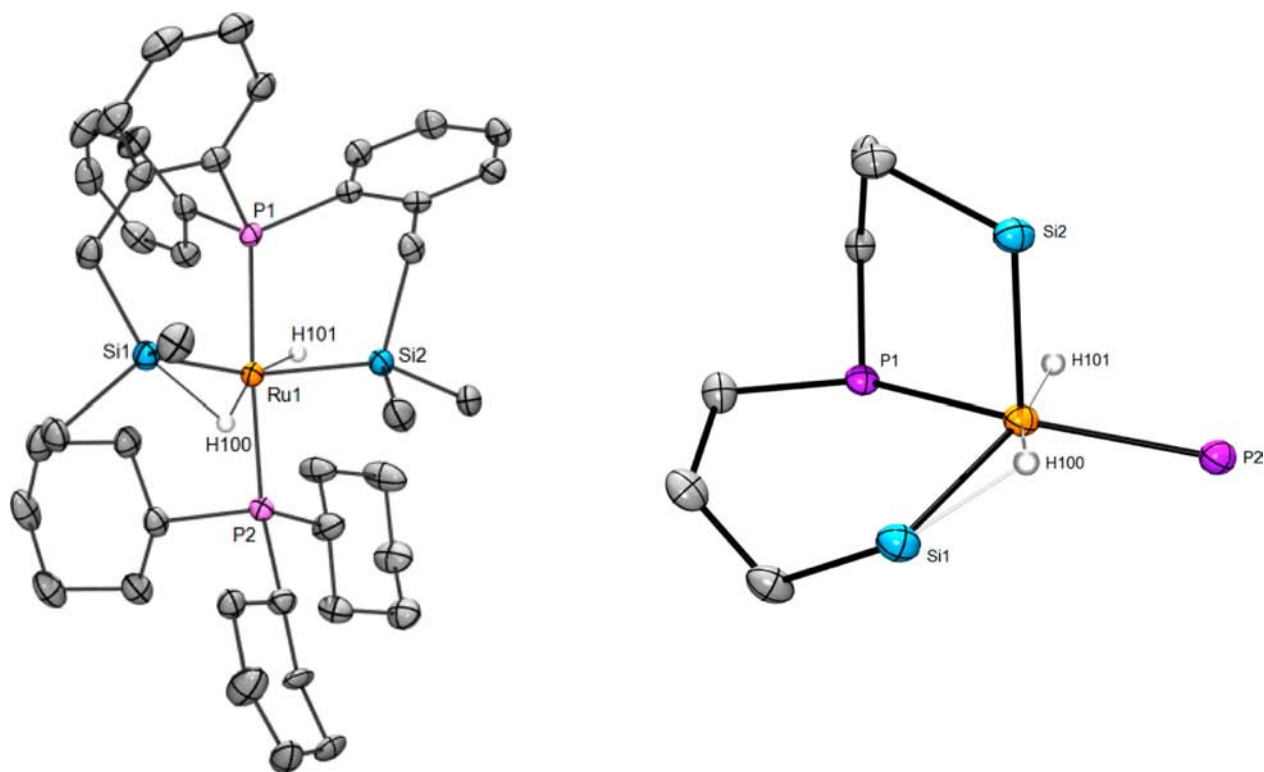
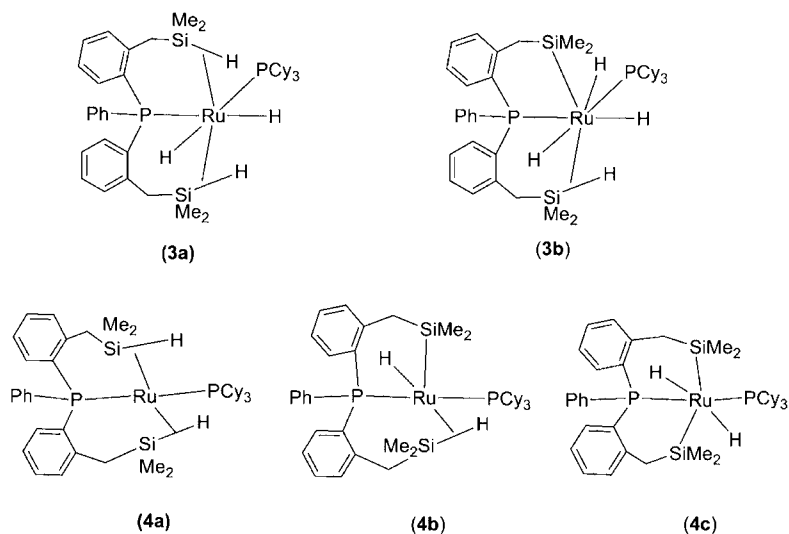


**Figure 2.** X-ray diffraction structure of 4 with thermal ellipsoids at the 50% probability level. Most hydrogen atoms were removed for clarity (left). View showing the square planar geometry around Ru when one considers the middle of the  $\eta^2$ -(Si1–H100) ligand as a single coordination point. The vacant coordination site lies trans to Si2. Most hydrogen and carbon atoms were removed for clarity (right).

temperature.<sup>27</sup> The dynamics of hydride/ $\eta^2$ -Si–H exchange have been previously described as accounting for stereochemical nonrigidity of the systems. In our case, the value of 40 Hz measured for the  $J_{\text{Si-H}}$  coupling in conjunction with the observed fluxionality of 3 in solution points to the existence of nonclassical  $\eta^2$ -SiH character in at least one but probably the two Si moieties, therefore supporting formulation 3a. The rapid exchange between the four hydride ligands (Ru–H and Ru–H–Si) of 3 in solution, evidenced by their equivalency on the NMR time scale at all accessible temperatures, is thus associated with a very low activation barrier. However, the situation is not clear-cut, and the contribution of structure 3b

cannot be utterly ruled out. This is reminiscent of what we have shown previously in the case of the phosphinosilane ligand  $\text{PPh}_2\text{CH}_2\text{OSiMe}_2\text{H}$ , which can coordinate to ruthenium via two different extreme modes: full oxidative addition and nonclassical sigma Si–H. A continuum between these two modes was proposed to be present in solution.<sup>13</sup>

**Dihydrogen Loss Leading to  $[\text{RuH}\{\eta^2\text{-(HSiMe}_2\text{)-CH}_2\text{-o-C}_6\text{H}_4\}]\text{PPh}[\text{CH}_2\text{-o-C}_6\text{H}_4\text{SiMe}_2](\text{PCy}_3)]$  (4). NMR Observation of a  $^{29}\text{Si}$  Decoalescence Process.** Despite complex 3 being stable over prolonged periods in solution at  $T \leq 288$  K, attempts at vacuum drying of benzene- $d_6$  solutions resulted in partial formation of a new complex 4. Indeed, when pure

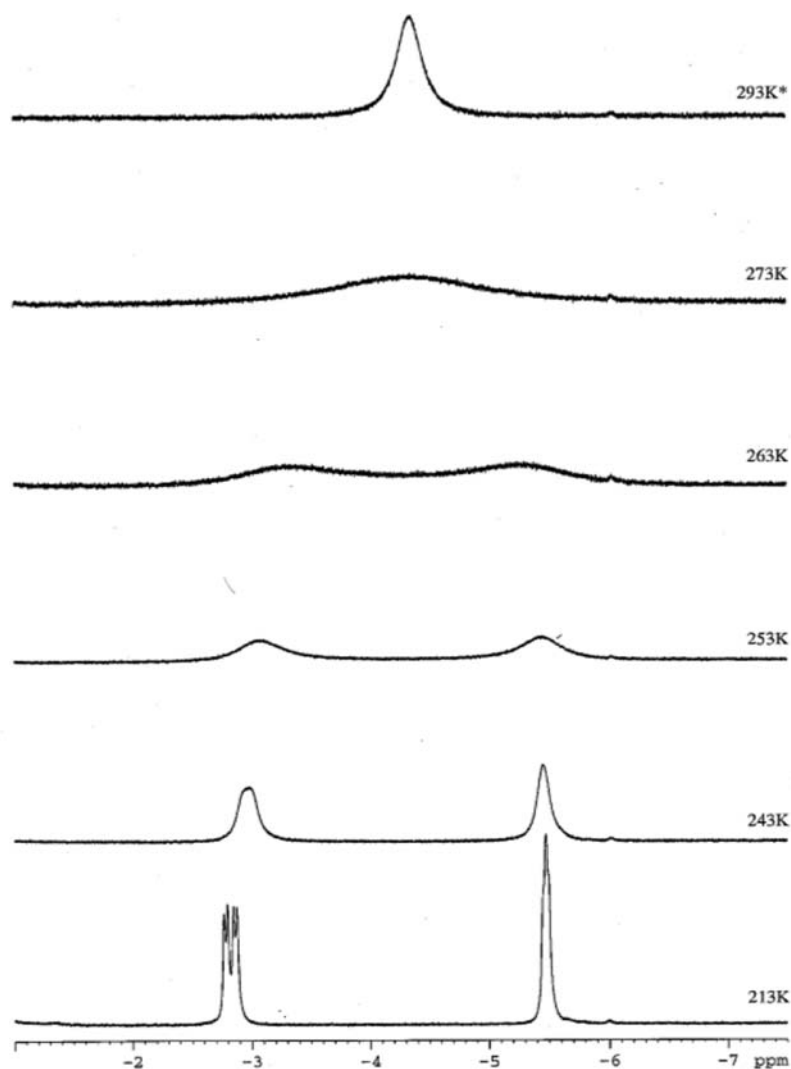


**Figure 3.** High field region of the  $^1\text{H}$  NMR spectrum (toluene- $d_6$ , 400 MHz) of **4** at varying temperatures showing decoalescence at 273 K.

crystals of **3** were exposed for 15 min to dynamic vacuum and redissolved, a 3:4 molar ratio was determined by NMR integration as 1:0.5. Complex **3** was quantitatively regenerated at ambient temperature under a pressure of 1–3 bar  $\text{H}_2$ . Keeping THF solutions of **3** at 308 K over 7 days yielded complex **4** in 90% isolated yield from **3**. Slow hexane diffusion into THF solutions of either in situ generated **3** kept at 308 K or of mixtures containing **3** and **4** in an initial 1:0.5 molar ratio at 238 K resulted in the growth of crystals of **4** suitable for X-ray diffraction analysis.

Thus, complex **3** undergoes reversible loss of dihydrogen leading to the formation of an orange 16-electron Ru(II) complex **4**,  $[\text{RuH}\{\eta^2\text{-(HSiMe}_2\text{)-CH}_2\text{-}o\text{-C}_6\text{H}_4\}\text{PPh}[\text{CH}_2\text{-}o\text{-C}_6\text{H}_4\text{SiMe}_2]\text{]}(\text{PCy}_3)]$  (Scheme 2), as characterized by X-ray diffraction and multinuclear NMR spectroscopy. To depict **4**, three arrested structures could be envisaged (Scheme 3). In **4a**, the two Si–H bonds would be coordinating to Ru in a nonclassical fashion giving rise to a formally 16-electron Ru(0) compound; in **4b**, oxidative addition of one Si–H bond would generate a hydrido(silyl)( $\eta^2\text{-Si-H}$ ) Ru(II) species prone to exhibiting SISHA interactions; finally, in **4c**, full oxidative addition of both Si–H bonds would render a Ru(IV) dihydride(disilyl) formulation. The molecular structure of **4** is shown in Figure 2, and relevant bond distances and angles are

presented in Table 1. It confirms a structure relatively close to that of complex **3** bearing only two hydrogen atoms in the coordination sphere of ruthenium. The findings discussed below in the solid state are in agreement with a structure nearer to proposed formulation **4b** in which one hydride is terminal, while the other one is involved in a  $\eta^2\text{-Si-H}$  interaction. Considering the centroid of the  $\eta^2\text{-Si-H}$  bond as a coordination point, the ruthenium is in a distorted square planar pyramid with the silyl in the apical position (Si2), the phosphorus atoms in the square planar base approximately *trans* to each other, exhibiting a P–Ru–P angle of  $154.37(3)^\circ$  much larger than that found in **3** of  $113.32(5)^\circ$ . The Si–Ru–Si angle is rather acute at  $104.50(4)^\circ$  by comparison to the corresponding angle in **3** accounting for  $112.36(5)^\circ$ . One of the silicon atoms exhibits an elongated Si1–H100 bond distance of  $1.71(3) \text{ \AA}$  as well as a Ru–Si1 distance of  $2.473(1) \text{ \AA}$ , both consistent with the  $\eta^2\text{-Si-H}$  formulation.<sup>23,29,31,34</sup> The other silicon atom bond distance to ruthenium, Ru–Si2, is by comparison shorter at  $2.324(1) \text{ \AA}$  in agreement with a silyl formulation. It is noteworthy that the distances between Si2 and the hydrogen atoms H100 and H101 are nonbonding ( $>2.6 \text{ \AA}$ ). The vacant site is *trans* to the strongest *trans* director Si2. Differential functional theory (DFT) calculations show an excellent agreement with the experimental values. In particular,

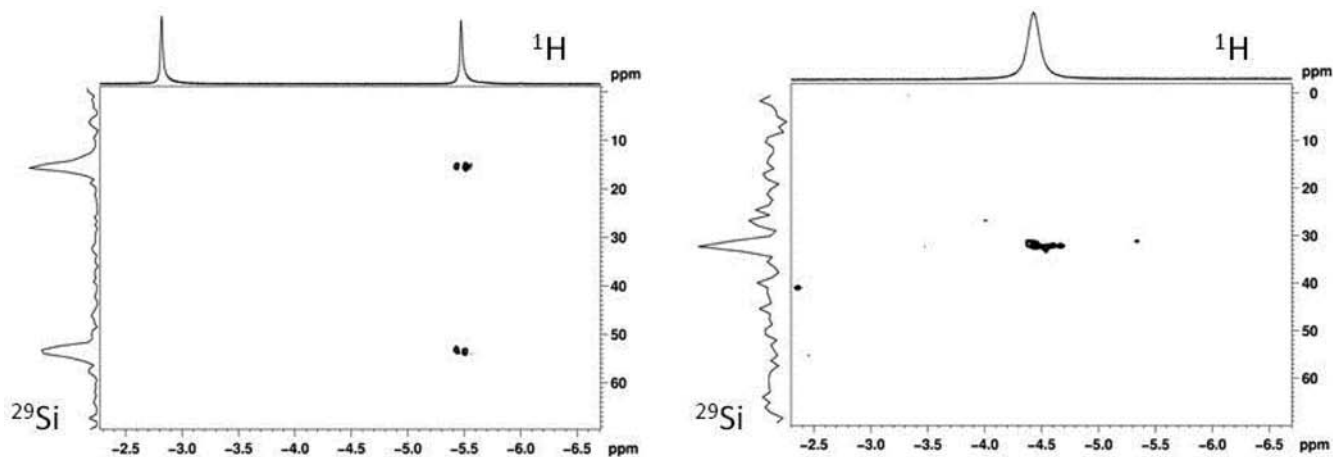


**Figure 4.** Region of the HMQC  $^1\text{H}-^{29}\text{Si}\{^{31}\text{P}\}$  NMR experiment at 324 K showing correlation of the silicon signal to the hydride resonance (H and H-Si), the two silicon, and the two hydrogen atoms around the ruthenium in complex **4** being in fast exchange (right). Region of the HMQC  $^1\text{H}-^{29}\text{Si}\{^{31}\text{P}\}$  NMR experiment at 213 K showing correlation of both silicon signals of **4** to only one high field  $^1\text{H}$  resonance (H-Si) with the same  $J_{\text{Si-H}}$  of 37 Hz (left).

two different Ru-Si bond distances were computed Ru-Si1 2.523 Å (exptl. 2.473(1) Å) and Ru-Si2 2.352 Å (exptl. 2.324(1) Å) as well as different extents of Si-H bond activation: the Si1-H100 bond distance, 1.763 Å, is typical of an  $\eta^2$ -Si-H bond, notably shorter than the nonbonding Si2...H100 and Si2...H101 distances (>2.6 Å). Thus, in the solid state, **4** appears to be formally a 16-electron Ru(II) species close to proposed structure **4b**.

At room temperature, the  $^1\text{H}$  NMR spectrum of **4** in toluene- $d_8$  solution shows in the hydride region a broad signal at  $\delta$  -4.34 (Figure 3). Decoalescence is observed at 273 K and two signals in a 1:1 integration ratio are seen at  $\delta$  -2.82 (dd,  $^2J_{\text{PH}}$  39.6 and 14 Hz) and  $\delta$  -5.47 (br) at the low temperature limit (213 K) (Figure 3). These rather low chemical shift values might be surprising but are in the range found for *trans* dihydride ruthenium species.<sup>35,36</sup> In our system, the hydride and the hydrogen attached to silicon (H-Si) are roughly in *trans* position as determined in the solid state by X-ray diffraction as well as by DFT. The exchange between the two types of hydrogen, Ru-H and Ru- $\eta^2$ -Si-H, is thus blocked and characterized by a  $\Delta G^\ddagger = 48.5 \text{ kJ mol}^{-1}$ , a value close to those previously reported for Si-H/Ru-H exchanges in bis(silane) complexes (47.5  $\text{kJ mol}^{-1}$  to 68.4  $\text{kJ mol}^{-1}$ ).<sup>27</sup> The  $^{31}\text{P}\{^1\text{H}\}$  NMR spectrum shows two inequivalent phosphines giving rise to an AX spin pattern with two doublets at  $\delta$  35 (phosphinodi(benzylsilane) ligand) and  $\delta$  53 (coordinated PCy<sub>3</sub>) exhibiting a  $^2J_{\text{P-P}}$  coupling constant of 177 Hz. This value is by comparison 46% larger than that of **3** and in accordance with a significantly larger P-Ru-P angle, which compensates for the unsaturated electronic character of **4**. This increased coupling is a strong indicator of the preservation in solution of the solid state structure for the heavy atoms.

The  $^{29}\text{Si}\{^{31}\text{P}\}\{^1\text{H}\}$  NMR (99.4 MHz) spectrum shows a broad singlet at  $\delta$  33 at 293 K for the two silicon atoms. At 324 K, broadening is reduced and a HMQC  $^1\text{H}-^{29}\text{Si}\{^{31}\text{P}\}$  experiment shows clearly the correlation between the  $^{29}\text{Si}$  signal at  $\delta$  33 and the  $^1\text{H}$  signal at  $\delta$  -4.4 (Figure 4 right). At the low temperature limit (213 K), the unique  $^{29}\text{Si}$  signal gives rise to two resonances at  $\delta$  54 and  $\delta$  16. A HMQC  $^1\text{H}-^{29}\text{Si}\{^{31}\text{P}\}$  experiment at 213 K shows the correlation of both silicon signals with only the  $^1\text{H}$  resonance at highest field ( $\delta$  -5.47,

Figure 4 left). For each silicon atom, the magnitude of the apparent  $J_{\text{Si-H}}$  coupling constant is 37 Hz. In contrast, the hydride signal at  $\delta$  -2.82 does not correlate to any of the two silicon signals. It was impossible to measure directly any  $^{29}\text{Si}$  signals from 293 to 213 K due in particular to small  $T_2$  values. This prevented the determination of the  $^{29}\text{Si}$  coalescence temperature, which should be close to room temperature. To our knowledge, the observation of a  $^{29}\text{Si}$  NMR decoalescence is unprecedented in silane complexes.<sup>23</sup>

Furthermore, DFT calculations gave the free energy of reaction  $\Delta_r G = +16.9 \text{ kJ mol}^{-1}$  (298 K) for the conversion of **3** to **4** + H<sub>2</sub>. Such a low value is in accordance with the facile transformation under experimental conditions. The process is assisted by a very facile isomerization of **3cis** (the DFT model of **3**) to a species **3trans** featuring *trans* phosphines (P1-Ru-P2 150.5°) only 3  $\text{kJ mol}^{-1}$  higher in energy than the *cis* isomer (see Supporting Information, Table S2). From **3trans**, H<sub>2</sub> release leading to **4**, featuring also the two phosphorus in *trans* disposition, is then facile.

The exchange of the two hydrogen atoms around the ruthenium (Ru-H and Ru-H-Si) is characterized by a barrier of 48.5  $\text{kJ mol}^{-1}$ , as determined by  $^1\text{H}$  NMR at 273 K. A much more unusual observation of a decoalescence process by  $^{29}\text{Si}$  NMR could be demonstrated. Hydride exchange is blocked at 213 K, and decoalescence of the  $^{29}\text{Si}$  signal observed at  $\delta$  32 at 324 K gives rise to two signals at  $\delta$  53 and  $\delta$  16. Most noteworthy, both these two signals correlate with only the highest field  $^1\text{H}$  signal ( $\delta$  -5.47) and with the same  $J_{\text{Si-H}}$  (37 Hz). We propose that this behavior is consistent with the intermediacy of a Si...H...Si bond interaction through a  $\sigma$ -CAM mechanism.<sup>37</sup> A simple rationalization would be a structure in which only one hydrogen lies in between the two silicons with the other being too far away to be involved in a  $\sigma$ -CAM process. The RuH/Ru-H-Si positions could be easily interchanged until the process is frozen at low temperature as demonstrated both by  $^1\text{H}$  and  $^{29}\text{Si}$  NMR. The rather different chemical shifts observed in the  $^{29}\text{Si}$  NMR spectra at the low temperature limit, namely,  $\delta$  54 and  $\delta$  16, are consistent with an arrested structure with two Si atoms in different chemical environments as shown in the solid state by X-ray diffraction.

We have recently reported a series of silazane complexes exhibiting a range of multicenter Ru-H-Si bonds, and in

several cases the Si...H...Si interaction was evidenced by different techniques but the silicon atoms could never be discriminated by NMR.<sup>38</sup> It should also be noted that our findings are reminiscent of the transition metal-free polyagostic Si–H–Si interactions reported in a series of silylium ions derived from polysilyl-substituted benzenes.<sup>39</sup>

## CONCLUSIONS

We have synthesized a novel pincer-like phosphinodi-(benzylsilane) ligand that allows for the isolation of ruthenium complexes exhibiting terminal hydride/ $\eta^2$ -Si–H exchange processes. Complex **3** is best formulated as an 18-electron species stabilized by two rare high order  $\varepsilon$ -agostic Si–H interactions with additional SISHA interactions. **3** can readily, and reversibly, lose dihydrogen to produce the 16-electron complex **4**, featuring a <sup>29</sup>Si NMR decoalescence, which to the best of our knowledge has never been reported in silane complex chemistry. The free energy  $\Delta_r G_{298}$  of the reaction of **3** to **4** + H<sub>2</sub> is only +16.9 kJ mol<sup>-1</sup> accounting for the facile conversion observed experimentally at 308 K. Our study shows that the phosphinodi(benzylsilane) can act as a “cooperating” ligand accommodating different coordination modes at a metal center through different extents of Si–H bond activation. These first results show great promise for the development of a new coordination chemistry with this pincer-like phosphinodi-(benzylsilane) ligand, and we are currently exploring its reactivity with other metal precursors. Catalytic studies are also underway and will be reported in due course.

## EXPERIMENTAL SECTION

**General Considerations.** All experiments were performed under argon atmosphere using standard Schlenk methods or in MBraun glove boxes. THF, toluene, hexane, and pentane were either dried and distilled from sodium using benzophenone ketyl as indicator or purified over a MBraun column system. In either case, they were degassed prior to use. Benzene-*d*<sub>6</sub> and toluene-*d*<sub>8</sub> were degassed via three freeze–pump–thaw cycles and stored over molecular sieves. Compound **2** was synthesized according to reported procedures.<sup>40</sup> Nuclear magnetic resonance spectra were recorded on Bruker AV 300, 400, 500, Varian Inova 400 MHz, and Varian NMRS-700 MHz spectrometers. Infrared spectra were recorded on a Bruker Alpha FT-IR spectrometer equipped with a Platinum single reflection ATR module. Microanalyses were performed at the Laboratoire de Chimie de Coordination on a Perkin-Elmer 2400 Series II analyzer or at UAEM on an Elementar Vario EL III instrument.

**Synthesis of PhP{(o-C<sub>6</sub>H<sub>4</sub>CH<sub>2</sub>)SiMe<sub>2</sub>H}<sub>2</sub>, **1**.** The phosphine PhP(*o*-tolyl)<sub>2</sub> was made *in house* from the reaction of 2 equiv of BrMg(*o*-C<sub>6</sub>H<sub>4</sub>CH<sub>3</sub>) and 1 equiv of PhPCl<sub>2</sub>. Indeed, 10 g (58.5 mmol) of Br(*o*-C<sub>6</sub>H<sub>4</sub>CH<sub>3</sub>) in THF was added dropwise to activated Mg (1.45 g, 58.5 mmol), and the reaction mixture was left to react at reflux temperature until the full consumption of the activated magnesium. Addition of Cl<sub>2</sub>PPh (4 mL, 29.2 mmol) and stirring for 24 h left a yellow solution and a white precipitate of MgBrCl which was separated by filtration. To the solution, ice (2 g) was added followed by 100 mL of a 0.5 M aqueous NH<sub>4</sub>Cl solution. The product was extracted twice with 50 mL of ethyl ether using a separating funnel. The ethereal phase was collected, dried over MgSO<sub>4</sub>, and finally evaporated to dryness. The yellowish powder was further purified by recrystallization from hot ethanol solutions at 273 K to yield a white solid in 75%, its purity verified by mp and <sup>1</sup>H and <sup>31</sup>P NMR. PhP{(o-C<sub>6</sub>H<sub>4</sub>CH<sub>3</sub>)<sub>2</sub> (2 g, 6.9 mmol) was dissolved in 30 mL of hexane, TMEDA (2.1 mL, 13.8 mmol) and titrated *n*BuLi (13.8 mmol) were added. After being stirred for 16 h, the bright orange reaction mixture was cooled to –78 °C, and ClSiMe<sub>2</sub>H (3 mL, 27.5 mmol) was added via syringe. The off-white suspension was allowed to warm up to room temperature and kept under stirring for 12 h, after which the solvent was removed by

distillation under a reduced pressure. The oily residue was redissolved in 50 mL of a 9:1 hexane/toluene mixture and transferred by cannula to a frit containing silica. The filtrate was dried under a vacuum yielding an opaque viscous liquid. Yield 83% from PhP{(o-C<sub>6</sub>H<sub>4</sub>CH<sub>3</sub>)<sub>2</sub>. <sup>1</sup>H NMR (C<sub>6</sub>D<sub>6</sub>, 700 MHz, 293 K):  $\delta$  [0.04 (dd,  $J_{\text{HH}} = 3.5$  Hz, 1.4 Hz, SiMe<sub>2</sub>) + 0.05 (dd,  $J_{\text{HH}} = 3.5$  Hz, 1.4 Hz, SiMe<sub>2</sub>)] = 12H]; [2.44 (d,  $J_{\text{HH}} = 3.5$  Hz, CH<sub>2</sub>) + 2.44 (d,  $J_{\text{HH}} = 3.5$  Hz, CH<sub>2</sub>)] = 4H], 4.22 (m, 2H,  $J_{\text{SiH}} = 196$  Hz,  $J_{\text{HH}} = 3.5$  Hz, SiH), 6.82 (t,  $J = 7$  Hz, 2H, aromatic), 7.02 (m, 9H, aromatic), 7.35 (tm,  $J = 7$  Hz, 2H, aromatic). <sup>31</sup>P{<sup>1</sup>H} (C<sub>6</sub>D<sub>6</sub>, 80.96 MHz, 293K):  $\delta$  –21.1 (s). <sup>13</sup>C{<sup>1</sup>H} (C<sub>6</sub>D<sub>6</sub>, 176.008 MHz, 293K):  $\delta$  –4.27 (d,  $J_{\text{CP}} = 2.1$  Hz, SiCH<sub>3</sub>), –4.18 (d,  $J_{\text{CP}} = 2.1$  Hz, SiCH<sub>3</sub>), 23.22 (d,  $J_{\text{CP}} = 20.4$  Hz, CH<sub>2</sub>), 124.98 (s, CHarom), 128.44 (d,  $J_{\text{CP}} = 3.3$  Hz, CHarom), 128.49 (s, CHarom), 128.75 (s, CHarom), 128.99 (d,  $J_{\text{CP}} = 4.9$  Hz, CHarom), 134.09 (d,  $J_{\text{CP}} = 19.5$  Hz, CHarom), 134.11 (s,  $C_{\text{ipso}} \text{ arom}$ ), 134.22 (s, CHarom), 136.95 (d,  $J_{\text{CP}} = 10.9$  Hz,  $C_{\text{ipso}} \text{ arom}$ ), 145.17 (d,  $J_{\text{CP}} = 26.9$  Hz,  $C_{\text{ipso}} \text{ arom}$ ). <sup>29</sup>Si{<sup>1</sup>H} NMR (CDCl<sub>3</sub>, 79.46 MHz, 293K):  $\delta$  –11.5 (s). IR (C<sub>6</sub>D<sub>6</sub>): 2118 cm<sup>-1</sup> ( $\nu$ , SiH), 1259 cm<sup>-1</sup> ( $\nu$ , SiMe<sub>2</sub>). Anal. Calcd for C<sub>24</sub>H<sub>31</sub>PSi<sub>2</sub>: C 70.88, H 7.68. Found: C 71.21, H 7.84. MS (EI+): *m/z* 405 (M<sup>+</sup> – 1H, 10), 391 (M<sup>+</sup> – CH<sub>3</sub>, 22), 256 (M<sup>+</sup> – C<sub>6</sub>H<sub>4</sub>CH<sub>2</sub>SiMe<sub>2</sub>H – 1H, 70).

**Synthesis of [RuH<sub>2</sub>{ $\eta^2$ -(HSiMe<sub>2</sub>)-CH<sub>2</sub>-o-C<sub>6</sub>H<sub>4</sub>]<sub>2</sub>PPh(PCy<sub>3</sub>)]<sub>2</sub>, **3**.** Compound **1** (130 mg, 0.32 mmol) was dissolved in approximately 1 mL of either C<sub>6</sub>D<sub>6</sub> or toluene-*d*<sub>8</sub> and added to complex **2** (255 mg, 0.38 mmol) at 298 K in a Fischer–Porter vessel inside the glovebox. Immediate evolution of gas was observed, and the sample was left to stir for 1 h. The contents were then put under 3 bar of H<sub>2</sub> gas and left at room temperature. Crystals suitable for X-ray diffraction were obtained after one week in these conditions. Yield 90%. For spectroscopic characterization they were filtered off and dried under a current of dihydrogen gas. <sup>1</sup>H NMR (C<sub>6</sub>D<sub>6</sub>, 300 MHz, 293K):  $\delta$  –9.02 (br, 4H, Ru–H/ $\sigma$ Si–H), 0.48 (br s, 6H, CH<sub>3</sub>), 0.64 (br s, 6H, CH<sub>3</sub>), 1.08–1.95 (m, 33H, PCy<sub>3</sub>), 2.41 (br s, 4H, CH<sub>2</sub>), 6.59–7.57 (m, 11H, arom), 8.03 (m, 2H, arom). Diastereotopic methylene protons were undistinguishable. <sup>31</sup>P{<sup>1</sup>H} NMR (C<sub>6</sub>D<sub>6</sub>, 121.44 MHz, 293 K):  $\delta$  29.6 (d,  $J_{\text{PP}} = 121$  Hz, PCy<sub>3</sub>),  $\delta$  68.3 (d,  $J_{\text{PP}} = 121$  Hz, P ligand **1**). <sup>13</sup>C{<sup>1</sup>H} (toluene-*d*<sub>8</sub>, 125.81 MHz, 263K):  $\delta$  11.25 (s, SiCH<sub>3</sub>), 26.68 (s, PCy<sub>3</sub>, CH<sub>2</sub>), 27.75 (d,  $J_{\text{PC}} = 9.2$  Hz, PCy<sub>3</sub>, CH<sub>2</sub>), 30.36 (s, PCy<sub>3</sub>, CH<sub>2</sub>), 34.90 (br, PSi<sub>2</sub>, CH<sub>2</sub>), 35.18 (br, PCy<sub>3</sub>, CH), 124.17 (d, CHarom), 129.02 (d,  $J_{\text{CP}} = 3$  Hz, CHarom), 129.26 (br s, CHarom), 130.14 (br s, CHarom), 130.94 (br, CHarom), 134.90 (br,  $C_{\text{ipso}} \text{ arom}$ ), 136.50 (d,  $J_{\text{CP}} = 1.3$  Hz,  $C_{\text{ipso}} \text{ arom}$ ), 136.83 (s, CHarom), 136.91 (s, CHarom), 145.53 (br,  $C_{\text{ipso}} \text{ arom}$ ). <sup>29</sup>Si{<sup>31</sup>P} NMR (toluene-*d*<sub>8</sub>, 99.325 MHz, 273K):  $\delta$  –0.7 ( $J_{\text{Si-H app}} = 40$  Hz). IR: 1997 cm<sup>-1</sup> ( $\nu$ , RuHSi and RuH), 1873 cm<sup>-1</sup> (m,  $\nu$ , RuHSi and RuH), 1811 cm<sup>-1</sup> (w,  $\nu$ , RuHSi and RuH).

**Synthesis of [RuH{ $\eta^2$ -(HSiMe<sub>2</sub>)-CH<sub>2</sub>-o-C<sub>6</sub>H<sub>4</sub>]<sub>2</sub>PPh[CH<sub>2</sub>-o-C<sub>6</sub>H<sub>4</sub>SiMe<sub>2</sub>]<sub>2</sub>(PCy<sub>3</sub>)]<sub>2</sub>, **4**.** The reaction of compound **1** (130 mg, 0.32 mmol) and complex **2** (260 mg, 0.39 mmol) was performed in a mixture of THF (approximately 1 mL) and hexane (approx. 0.3 mL). The contents were degassed by two cycles of freeze–pump–thaw with liquid nitrogen and kept under a vacuum at 298 K in a Schlenk tube for ca. two weeks. The orange crystals were filtered off, washed three times with cold hexane, and dried under a vacuum. Yield: 76% from **2**. Alternatively, keeping THF solutions of **3** at 308 K over 7 days yielded complex **4** in 90% isolated yield. <sup>1</sup>H NMR (toluene-*d*<sub>8</sub>, 500 MHz, 293 K): –4.34 (br, 2H, RuH and RuHSi); 0.40 (br, 12H, SiMe<sub>2</sub>); [0.85–2.1 (m, PCy<sub>3</sub>, overlapping with CH<sub>2</sub>) + 2.07 (m, overlapping with PCy<sub>3</sub>, CH<sub>2</sub>)] = 35H]; 2.22 (dd,  $J = 5, 10$  Hz, 2H, CH<sub>2</sub>), 6.89–7.96 (m, 13H, arom). Diastereotopic methyl groups were undistinguishable. <sup>1</sup>H NMR (toluene-*d*<sub>8</sub>, 500 MHz, 213 K):  $\delta$  –2.82 (dd,  $J_{\text{H-PCy}_3} = 39.6$  and  $J_{\text{H-PSi}_2} = 14$  Hz, 1H, RuH101), –5.47 (pseudo t,  $J_{\text{H-PCy}_3} = 14$  Hz,  $J_{\text{H-PSi}_2} = 6.7$  Hz, 1H, RuH100Si). The assignment was made upon selective <sup>31</sup>P NMR decoupling experiments. <sup>31</sup>P{<sup>1</sup>H} NMR (toluene-*d*<sub>8</sub>, 202.54 MHz, 213 K):  $\delta$  35.0 (d,  $J_{\text{PP}} = 177$  Hz, PSi<sub>2</sub>), 53.1 (d,  $J_{\text{PP}} = 177$  Hz, PCy<sub>3</sub>). <sup>29</sup>Si{<sup>31</sup>P}(toluene-*d*<sub>8</sub>, 99.40 MHz, 324 K):  $\delta$  32 (br, correlation with the –4.4 <sup>1</sup>H signal). <sup>29</sup>Si{<sup>31</sup>P}(toluene-*d*<sub>8</sub>, 99.40 MHz, 213 K):  $\delta$  54 (br,  $J_{\text{H100-Si}} = 37$  Hz), 16 (br,  $J_{\text{H100-Si}} = 37$  Hz). <sup>13</sup>C{<sup>1</sup>H} (toluene-*d*<sub>8</sub>, 125.81 MHz, 293 K):  $\delta$  8.38 (s, SiCH<sub>3</sub>), 9.62 (s, SiCH<sub>3</sub>), 26.45 (s, PCy<sub>3</sub>, CH<sub>2</sub>), 27.41 (d,  $J_{\text{CP}} = 10.1$  Hz, PCy<sub>3</sub>, CH<sub>2</sub>), 29.64 (s,

PCy<sub>3</sub>, CH<sub>2</sub>), 34.17 (d, <sup>3</sup>J<sub>CP</sub> = 21.4 Hz, PSi<sub>2</sub>, CH<sub>2</sub>), 35.94 (br, PCy<sub>3</sub>, CH), 127.88 (br s, CH<sub>arom</sub>), 128.16 (br s, CH<sub>arom</sub>), 129.02 (s, CH<sub>arom</sub>), 129.43 (s, CH<sub>arom</sub>), 129.99 (d, J<sub>CP</sub> = 6.29 Hz, CH<sub>arom</sub>), 130.20 (s, CH<sub>arom</sub>), 134.19 (s, C<sub>ipso</sub> arom), 134.82 (d, J<sub>CP</sub> = 7.5 Hz, C<sub>ipso</sub> arom), 147.48 (d, J<sub>CP</sub> = 15.1 Hz, C<sub>ipso</sub> arom). IR: 1808 cm<sup>-1</sup> (w,  $\nu$ RuHSi and RuH). Anal. Calcd for C<sub>42</sub>H<sub>64</sub>P<sub>2</sub>Si<sub>2</sub>Ru: C 64.02, H 8.19. Found: C 63.90, H 8.11.

## X-RAY DATA

Important crystallographic data are given in Table 2; the experimental procedure and relevant data are in the Supporting Information as CIF data (also deposited at the CCDC: No. 929314 (3), No. 929315 (4)).

**Table 2. Crystal Data for Compounds 3 and 4**

	3	4
formula	C <sub>84</sub> H <sub>132</sub> P <sub>4</sub> Ru <sub>2</sub> Si <sub>4</sub>	C <sub>42</sub> H <sub>64</sub> P <sub>2</sub> RuSi <sub>2</sub> ·2(C <sub>4</sub> H <sub>8</sub> O)
formula weight	1580.28	932.33
cryst syst	monoclinic	triclinic
space group	P2 <sub>1</sub> /c (No. 14)	P $\bar{1}$ (No. 2)
a, Å	37.6275(15)	10.0343(19)
b, Å	10.4778(3)	13.224(3)
c, Å	20.726(5)	19.052(4)
$\alpha$ , deg	90	99.247(3)
$\beta$ , deg	97.930(3)	95.585(3)
$\gamma$ , deg	90	103.004(3)
V, Å <sup>3</sup>	8093(2)	2407.7(9)
Z	4	2
calcd density (g/cm <sup>3</sup> )	1.297	1.286
$\mu$ , mm <sup>-1</sup>	0.554	0.479
F(000)	3360	996
crystal size, mm	0.02 × 0.10 × 0.17	0.16 × 0.21 × 0.28
temp, K	100	100
radiation, Å	Mo K $\alpha$ , 0.71073	Mo K $\alpha$ , 0.71073
$\theta$ min– $\theta$ max, deg	2.9, 24.7	1.6, 25.0
data set	–44:43; –12:12; –24:24	–11:11; –15:15; –22:22
tot., uniq data, R(int)	79609, 13787, 0.112	21875, 8440, 0.043
obsd data [I > 0.0 $\sigma$ (I)]	9681	7176
N <sub>ref</sub> , N <sub>par</sub>	13787, 855	8440, 615
R, wR <sub>2</sub> , S	0.0612, 0.1066, 1.08	0.0453, 0.1245, 1.05
min and max resd dens, e·Å <sup>-3</sup>	–0.88, 0.58	–0.71, 1.33

## COMPUTATIONAL DETAILS

DFT calculations were performed with the GAUSSIAN 03 series of programs<sup>41</sup> using the nonlocal hybrid functional denoted as B3PW91.<sup>42,43</sup> The ruthenium, phosphorus, and silicon atoms were represented by the relativistic effective core potential (RECP) from the Stuttgart group and their associated basis set,<sup>44,45</sup> augmented by polarization functions ( $\alpha_f = 1.235$ , Ru;  $\alpha_d = 0.387$ , P;  $\alpha_d = 0.284$  Si).<sup>46,47</sup> The remaining atoms (C, H) were represented by 6-31G(d,p) basis sets.<sup>48</sup> Full optimizations of geometry without any constraint were performed. Calculations of harmonic vibrational frequencies were performed to determine the nature of each extremum. Bond distances and angles data are reported in Table S1 for **3trans** and **3cis** and in Table S2 for **4** (Supporting Information).

## ASSOCIATED CONTENT

### Supporting Information

CIF data for complexes **3** and **4**. Computational details and Cartesian coordinates for the calculated structures. This

material is available free of charge via the Internet at <http://pubs.acs.org>.

## AUTHOR INFORMATION

### Corresponding Author

\*E-mail: [vmontiel@uaem.mx](mailto:vmontiel@uaem.mx) (V.M.P.), [sylviane.sabo@lcc-toulouse.fr](mailto:sylviane.sabo@lcc-toulouse.fr) (S.S.E.).

### Notes

The authors declare no competing financial interest.

## ACKNOWLEDGMENTS

This work was supported by CONACYT (Project 105762 and sabbatical grants), CNRS and Université Paul Sabatier (invited professorship to V.M.P. and M.A.M.H.). Computer time was given by the HPC resources of CALMIP (Toulouse, France) under the allocation 2012-[P0909]. Ms. Hanit Treviño is thanked for laboratory assistance and Dr. Yannick Coppel for recording <sup>29</sup>Si NMR spectra.

## REFERENCES

- Gunanathan, C.; Milstein, D. *Acc. Chem. Res.* **2011**, *44*, 588.
- Vogt, M.; Rivada-Wheelaghan, O.; Iron, M. A.; Leitius, G.; Diskin-Posner, Y.; Shimon, L. J. W.; Ben-David, Y.; Milstein, D. *Organometallics* **2013**, *32*, 300.
- (a) Collier, M. R.; Eaborn, C.; Jovanović, B.; Lappert, M. F.; Manojlović-Muir, L.; Muir, K. W.; Truelock, M. M. *J. Chem. Soc. Chem. Commun.* **1972**, 613. (b) Zhu, J.; Lin, Z.; Marder, T. B. *Inorg. Chem.* **2005**, *44*, 9384.
- (a) *The Chemistry of Pincer Compounds*; Morales-Morales, D.; Jensen, C., Eds.; Elsevier Science: Amsterdam, 2007. (b) Van Koten, G.; Milstein, D. *Top. Organomet. Chem.* **2013**, *40*, Special Issue on Organometallic Pincer Chemistry. (c) Albrecht, M.; Lindner, M. M. *Dalton Trans.* **2011**, *40*, 8733. (d) Van Koten, G.; Albrecht, M. *Angew. Chem., Int. Ed.* **2001**, *40*, 3750.
- Balakrishna, M. S.; Chandrasekaran, P.; George, P. P. *Coord. Chem. Rev.* **2003**, *241*, 87.
- Kameo, H.; Ishii, S.; Nakazawa, H. *Dalton Trans.* **2012**, *41*, 11386.
- (a) Holmes-Smith, R. D.; Osei, R. D.; Stobart, S. R. *J. Chem. Soc., Perkin Trans. I* **1983**, 861. (b) Joslin, F. L.; Stobart, S. *Inorg. Chem.* **1993**, *32*, 2221. (c) Gossage, R. A.; McLennan, G. D.; Stobart, S. R. *Inorg. Chem.* **1996**, *35*, 1729.
- Montiel-Palma, V.; Muñoz-Hernández, M. A.; Ayed, T.; Barthelat, J. C.; Grellier, M.; Vendier, L.; Sabo-Etienne, S. *Chem. Commun.* **2007**, 3963.
- (a) Morgan, E.; MacLean, D. F.; McDonald, R.; Turculet, L. *J. Am. Chem. Soc.* **2009**, *131*, 14234. (b) MacLean, D. F.; McDonald, R.; Ferguson, M. J.; Caddell, A. J.; Turculet, L. *Chem. Commun.* **2008**, 5146. (c) Mitton, S. J.; McDonald, R.; Turculet, L. *Organometallics* **2009**, *28*, 5122. (d) Ruddy, A. J.; Mitton, S. J.; McDonald, R.; Turculet, L. *Chem. Commun.* **2012**, *48*, 1159.
- Sangtrirutnugul, P.; Tilley, T. D. *Organometallics* **2008**, *27*, 2223.
- García-Camprubí, A.; Martín, M.; Sola, E. *Inorg. Chem.* **2010**, *49*, 10649.
- Suh, H.-W.; Schmeier, T. J.; Hazari, N.; Kemp, R. A.; Takase, M. *K. Organometallics* **2012**, *31*, 8225.
- Montiel-Palma, V.; Piechaczyk, O.; Picot, A.; Auffrant, A.; Vendier, L.; Le Floch, P.; Sabo-Etienne, S. *Inorg. Chem.* **2008**, *47*, 8601.
- Lee, Y.; Kinney, R. A.; Hoffman, B. M.; Peters, J. C. *J. Am. Chem. Soc.* **2011**, *133*, 16366.
- Sola, E.; García-Camprubí, A.; Andrés, J. L.; Martín, M.; Plou, P. *J. Am. Chem. Soc.* **2010**, *132*, 9111.
- Korshin, E. E.; Leitius, G.; Shimon, L. J. W.; Konstantinovski, L.; Milstein, D. *Inorg. Chem.* **2008**, *47*, 7177.
- (a) Mankad, N. P.; Whited, M. T.; Peters, J. C. *Angew. Chem., Int. Ed. Engl.* **2007**, *46*, 5768. (b) Lee, Y.; Mankad, N. P.; Peters, J. C.



- Nat. Chem.* **2010**, *2*, 558. (c) Takaoka, A.; Mankad, N. P.; Peters, J. C. *J. Am. Chem. Soc.* **2011**, *133*, 8440.
- (18) (a) Takaya, J.; Iwasawa, N. *Dalton Trans.* **2011**, *40*, 8814. (b) Takaya, J.; Kirai, N.; Iwasawa, N. *J. Am. Chem. Soc.* **2011**, *133*, 12980.
- (19) MacInnis, M. C.; MacLean, D. F.; Lundgren, R. J.; McDonald, R.; Turculet, L. *Organometallics* **2007**, *26*, 6522.
- (20) Takaoka, T.; Moret, M. E.; Peters, J. C. *J. Am. Chem. Soc.* **2012**, *134*, 6695.
- (21) (a) Li, Y.-H.; Zhang, Y.; Ding, X.-H. *Inorg. Chem. Commun.* **2011**, *14*, 1306. (b) Li, Y.-H.; Ding, X.-H.; Zhang, Y.; He, W.-R.; Huang, W. *Inorg. Chem. Commun.* **2012**, *15*, 194.
- (22) (a) Tobita, H.; Hasegawa, K.; Minglana, J. J. G.; Luh, L.-S.; Okazaki, M.; Ogino, H. *Organometallics* **1999**, *18*, 2058. (b) Okazaki, M.; Yamahira, N.; Minglana, J. J. G.; Tobita, H. *Organometallics* **2004**, *23*, 4531. (c) Minglana, J. J. G.; Okazaki, M.; Hasegawa, K.; Luh, L.-S.; Yamahira, N.; Komuro, T.; Ogino, H.; Tobita, H. *Organometallics* **2007**, *26*, 5859. (d) Tobita, H.; Yamahira, N.; Ohta, K.; Komuro, T.; Okazaki, M. *Pure Appl. Chem.* **2008**, *80*, 1155. (e) Komuro, T.; Tobita, H. *Chem. Commun.* **2010**, *46*, 1136.
- (23) (a) Corey, J. Y. *Chem. Rev.* **2011**, *111*, 863. (b) Corey, J. Y.; Braddock-Wilking, J. *Chem. Rev.* **1999**, *99*, 175.
- (24) Lachaize, S.; Vendier, L.; Sabo-Etienne, S. *Dalton Trans.* **2010**, *39*, 8492.
- (25) Wang, W.; Inoue, S.; Irran, E.; Driess, M. *Angew. Chem., Int. Ed. Engl.* **2012**, *51*, 3691.
- (26) Brück, A.; Gallego, D.; Wang, W.; Irran, E.; Driess, M.; Hartwig, J. F. *Angew. Chem., Int. Ed. Engl.* **2012**, *51*, 11478.
- (27) Delpéch, F.; Sabo-Etienne, S.; Daran, J.-C.; Chaudret, B.; Hussein, K.; Marsden, C. J.; Barthelat, J.-C. *J. Am. Chem. Soc.* **1999**, *121*, 6668.
- (28) Atheaux, I.; Delpéch, F.; Donnadiéu, B.; Sabo-Etienne, S.; Chaudret, B.; Hussein, K.; Barthelat, J.-C.; Braun, T.; Duckett, S. B.; Perutz, R. N. *Organometallics* **2002**, *21*, 5347.
- (29) Lachaize, S.; Sabo-Etienne, S. *Eur. J. Inorg. Chem.* **2006**, 2115.
- (30) (a) Duckett, S. B.; Haddleton, D. M.; Jackson, S. A.; Perutz, R. N.; Poliakov, M.; Upmacis, R. K. *Organometallics* **1988**, *7*, 1526. (b) Taw, F. L.; Bergman, R. G.; Brookhart, M. *Organometallics* **2004**, *23*, 886. (c) Peulecke, N.; Ohff, A.; Kosse, P.; Tillack, A.; Spannenberg, A.; Kempe, R.; Baumann, W.; Burlakov, V. V.; Rosenthal, U. *Chem.—Eur. J.* **1998**, *4*, 1852. (d) Ignatov, S. K.; Rees, N. H.; Merkoulou, A. A.; Dubberley, S. R.; Razuvaev, A. G.; Mountford, P.; Nikonov, G. I. *Chem.—Eur. J.* **2008**, *14*, 296.
- (31) Alcaraz, G.; Sabo-Etienne, S. *Coord. Chem. Rev.* **2008**, *252*, 2395.
- (32) Horbatenko, Y.; Vyboishchikov, S. F. *Organometallics* **2013**, *32*, 514.
- (33) Delpéch, F.; Sabo-Etienne, S.; Donnadiéu, B.; Chaudret, B. *Organometallics* **1998**, *17*, 4926.
- (34) Nikonov, G. I. *Adv. Organomet. Chem.* **2005**, *53*, 217.
- (35) Grellier, M.; Vendier, L.; Sabo-Etienne, S. *Angew. Chem., Int. Ed. Engl.* **2007**, *46*, 2613.
- (36) Abbel, R.; Abdur-Rashid, K.; Faatz, M.; Hadzovic, A.; Lough, A. J.; Morris, R. H. *J. Am. Chem. Soc.* **2005**, *127*, 1870.
- (37) Perutz, R. N.; Sabo-Etienne, S. *Angew. Chem. Int. Ed.* **2007**, *46*, 2578.
- (38) Smart, K. A.; Grellier, M.; Vendier, L.; Mason, S. A.; Capelli, S. C.; Albinati, A.; Sabo-Etienne, S. *Inorg. Chem.* **2013**, *52*, 2654.
- (39) (a) Khalimon, A. Y.; Lin, Z. H.; Simionescu, R.; Vyboishchikov, S. F.; Nikonov, G. I. *Angew. Chem., Int. Ed.* **2007**, *46*, 4530. (b) Tussupbayev, S.; Nikonov, G. I.; Vyboishchikov, S. F. *J. Phys. Chem. A* **2009**, *113*, 1199.
- (40) Borowski, A. F.; Sabo-Etienne, S.; Christ, M. L.; Donnadiéu, B.; Chaudret, B. *Organometallics* **1996**, *15*, 1427.
- (41) See ref 1 in Supporting Information for full reference.
- (42) Becke, A. D. *J. Chem. Phys.* **1993**, *98*, 5648.
- (43) Perdew, J. P.; Wang, Y. *Phys. Rev. B* **1992**, *45*, 13244.
- (44) Andrae, D.; Häussermann, U.; Dolg, M.; Stoll, H.; Preuss, H. *Theor. Chim. Acta* **1990**, *77*, 123.
- (45) Bergner, A.; Dolg, M.; Kuchle, W.; Stoll, H.; Preuss, H. *Mol. Phys.* **1993**, *80*, 1431.
- (46) Ehlers, A. W.; Böhme, M.; Dapprich, S.; Gobbi, A.; Höllwarth, A.; Jonas, V.; Köhler, K. F.; Stegmann, R.; Veldkamp, A.; Frenking, G. *Chem. Phys. Lett.* **1993**, *208*, 111.
- (47) Höllwarth, A.; Böhme, H.; Dapprich, S.; Ehlers, A. W.; Gobbi, A.; Jonas, V.; Köhler, K. F.; Stegmann, R.; Veldkamp, A.; Frenking, G. *Chem. Phys. Lett.* **1993**, *208*, 237.
- (48) Hariharan, P. C.; Pople, J. A. *Theor. Chim. Acta* **1973**, *28*, 213.